Quantification of Smoking-Induced Occupancy of β_2-Nicotinic Acetylcholine Receptors: Estimation of Nondisplaceable Binding

Irina Esterlis[1], Kelly P. Cosgrove[1], Jeffery C. Batis[1,2], Frederic Bois[1], Stephanie M. Stiklus[1], Evgenia Perkins[1], John P. Seibyl[2], Richard E. Carson[3], and Julie K. Staley[†1,2]

[1]Department of Psychiatry, Yale University School of Medicine and the Veteran's Affairs Connecticut Healthcare System (VACHS), West Haven, Connecticut; [2]Institute for Neurodegenerative Disorders, New Haven, Connecticut; and [3]Department of Diagnostic Radiology, Yale University School of Medicine and the Veteran's Affairs Connecticut Healthcare System (VACHS), West Haven, Connecticut

5-^{123}I-iodo-85380 (^{123}I-5-IA) is used to quantitate high-affinity nicotinic acetylcholine receptors (β_2-nAChRs) on human SPECT scans. The primary outcome measure is V_T/f_P, the ratio at equilibrium between total tissue concentration (free, nonspecifically bound, and specifically bound) and the free plasma concentration. Nondisplaceable uptake (free plus nonspecific) of ^{123}I-5-IA has not been measured in human subjects. Nicotine has high affinity for β_2*-nAChRs (nAChRs containing the β_2* subunit, for which * represents other subunits that may also be part of the receptor) and displaces specifically bound ^{123}I-5-IA. In this study, we measured nicotine occupancy and nondisplaceable binding in healthy smokers after they had smoked to satiety. **Methods:** Eleven nicotine-dependent smokers (mean age ± SD, 35.6 ± 14.4 y) completed the study. One subject was excluded from subsequent analyses because of abnormal blood nicotine levels. Subjects abstained from tobacco smoke for 5.3 ± 0.9 d and participated in a 15- to 17-h SPECT scanning day. ^{123}I-5-IA was administered by bolus plus constant infusion, with a total injected dose of 361 ± 20 MBq. At approximately 6 h after the start of the infusion, three 30-min SPECT scans and a 15-min transmission–emission scan were acquired to obtain baseline β_2*-nAChR availability. Subjects then smoked to satiety (2.4 ± 0.7 cigarettes), and arterial (first 40 min) and venous (until study completion) plasma nicotine and cotinine levels were collected. About 1 h after subjects had smoked to satiety, up to six 30-min SPECT scans were acquired. V_T/f_P data, computed from the tissue and plasma radioactivity measurements from the presmoking baseline and postsmoking scans, were analyzed using the Lassen plot method. **Results:** Receptor occupancy after subjects had smoked to satiety was 67% ± 9% (range, 55%–80%). Nondisplaceable uptake was estimated as 19.4 ± 5.8 mL·cm^{-3} (range, 15–28 mL·cm^{-3}). Thus, in the thalamus, where mean V_T/f_P is 93 mL·cm^{-3}, nondisplaceable binding represents approximately 20% of the total binding. **Conclusion:** These results are in agreement with previous findings and suggest that when satiating doses of nicotine are administered to smokers, imaging of receptor availability can yield valuable data, such as quantifiable measures of nondisplaceable binding.

Key Words: SPECT; 5-^{123}I-iodo-85380; smoking to satiety; human smokers

J Nucl Med 2010; 51:1226–1233
DOI: 10.2967/jnumed.109.072447

Nicotinic acetylcholine receptors (nAChRs) are abundant throughout the peripheral and central nervous systems, are the primary targets for nicotine in the brain, and play an important role in cognition and behavior. The nAChRs are pentameric ligand–gated ion channels. Many of the subunits have been identified, but nicotine has the highest affinity for nAChRs containing the β_2*-subunit (β_2*-nAChRs, for which * represents other subunits that may also be part of the receptor), which are the most widely expressed in the brain. Changes in ligand binding to the high-affinity state of β_2*-nAChRs have been demonstrated in tobacco smoking (*1,2*) and psychiatric and neurocognitive disorders including schizophrenia (*3,4*) and Alzheimer disease (*5,6*). In vivo imaging of β_2*-nAChRs has significantly advanced since the development of 3-[2(*S*)-2-azetidinylmethoxy]pyridine (A-85380) (*7*), which is used for SPECT when labeled with ^{123}I (*8*) or for PET when labeled with ^{18}F (*9,10*). A-85380 has a high affinity and low dissociation from the receptor–ligand complex, high specific-to-nonspecific binding ratio, and high selectivity for the β_2*-nAChR (*8,11*). Consistent with the known distribution of β_2*-nAChRs, A-85380 displays a high binding in the thalamus, an intermediate binding in the cortex and striatum (*12–14*), and the lowest binding in the cerebellum (*14,15*). 5-^{123}I-iodo-85380 (^{123}I-5-IA) is a halogenated analog of A-85380 (*16*) and is safe and nontoxic (*17,18*). Further, there is good agreement between bolus and bolus plus infusion paradigms using ^{123}I-5IA, indicating that quantitation of β_2*-nAChR

Received Nov. 4, 2009; revision accepted Mar. 19, 2010.
For correspondence or reprints contact: Irina Esterlis, Yale University School of Medicine and the Veteran's Affairs Connecticut Healthcare System (VACHS), 950 Campbell Ave., 116A6, West Haven, CT 06516.
E-mail: irina.esterlis@yale.edu
†Deceased.

availability using this ligand is accurate (*19*). Use of A-85380 has been verified in animal (*11,19,20*) and human (*17,21,22*) studies.

Our group has quantified β_2*-nAChR availability, measured with ^{123}I-5-IA SPECT, using V_T/f_p—which represents regional brain concentration (kBq/cm^3) divided by free parent concentration in plasma (f_p; kBq/mL) (*23,24*) and equals the sum of specific (V_S/f_p) and nondisplaceable (V_{ND}/f_p) binding. Specifically, we demonstrated significant individual variability in protein binding (*23*): observed sex differences in the volume of distribution were due to differences in protein binding of the radiotracer. Thus, it is critical to correct for free fraction (f_p) in our outcome measure and report V_T/f_p as opposed to V_T. However, by reporting V_T/f_p, we do not correct for V_{ND}/f_p. To obtain a more precise measure of β_2*-nAChR availability in vivo, an accurate measurement of nonspecific binding has to be made. The purpose of the present study was to estimate V_{ND}/f_p of ^{123}I-5-IA in human tobacco smokers by examining displacement through saturation of receptors by the amount of tobacco smoke required to reach satiety and applying a graphical analysis of the V_T/f_p change from baseline to estimate both occupancy and V_{ND}/f_p. In individuals who smoke, this can be done safely through self-administration of tobacco cigarettes to satiating levels (*25*). This study was conducted in smokers rather than nonsmokers so that participants could safely self-administer satiating levels of nicotine without adverse side effects such as the significant increase in blood pressure and disorientation (*26*), increased tension, confusion, and decreased vigor (*27,28*) that can occur in nicotine-naïve individuals after administration of a small dose of nicotine (such as from a nicotine patch). We calculated V_{ND}/f_p after smokers smoked to satiety, which has not been previously reported. We also examined associations between receptor occupancy and smoking parameters and hypothesized that greater receptor occupancy would be reached through smoking a greater number of cigarettes.

MATERIALS AND METHODS

Participants

Eleven volunteers (5 men and 6 women; mean age ± SD, 35.6 ± 14.4 y), who smoked 17.5 ± 6.8 cigarettes/d for 19.6 ± 14.2 y (Table 1), participated in the study. Nine subjects were Caucasian, 1 African American, and 1 Asian American. They provided written informed consent to participate in this study, conducted at Yale University and the West Haven Veteran's Affairs Connecticut Healthcare System; the study was approved by the Human Investigational Review Committees at both institutions. Eligibility was evaluated via structured interview, behavioral assessments, physical examination, laboratory blood tests, urine drug screen, and an electrocardiogram. None of the subjects had a recent history or evidence of a serious medical or neurologic illness, head trauma with significant loss of consciousness, psychiatric disorder, or substance abuse (except for nicotine dependence) as determined by the Structured Clinical Interview for the *Diagnostic and Statistical Manual of Mental Disorders,* 4th edition (*29*). Subjects had not used psychotropic substances other than alcohol for at least 1 y and had not used marijuana for at least 1 mo preceding the study. Women were not pregnant or breast-feeding. Nicotine dependence and current depressive symptoms were evaluated with the Fagerstrom Test of Nicotine Dependence, Center for Epidemiological Studies Depression Scale, and Beck Depression Inventory at intake and on the day of scanning.

Smoking Cessation

Two weeks before the SPECT scanning day, subjects met with research staff to learn tobacco smoking–abstinence techniques and set the date for smoking cessation. All subjects were asked to abstain from smoking for 4–6 d (mean ± SD, 5.3 ± 0.9 d) before the SPECT scanning day to allow time for residual nicotine to clear from the brain (*30*). Nonsmoking status was confirmed by breath carbon monoxide levels less than 11 pulses per minute and negligible plasma (≤100 ng/mL) and urinary (<200 ng/mL) cotinine levels on the scanning day.

MRI and ^{123}I-5-IA SPECT

MRI. Each subject participated in 1 MRI scan before SPECT. MRI was performed on a Signa 1.5-T system (GE Healthcare). Axial images parallel to the anteroposterior commissural line were acquired with the following parameters: echo time, 5 ms; repetition time, 24 ms; matrix, 256 × 192; number of excitations, 1; field of view, 24 cm; and 128 contiguous slices with 1.3-mm thickness.

SPECT. All emission scans were obtained on a Prism 3000 XP (Picker), a 3-head SPECT camera equipped with a low-energy, ultra-high-resolution fanbeam collimator (photopeak window, 159 keV ± 10%; matrix, 128 × 128) with a uniform sensitivity across the field of view. A ^{57}Co-distributed source was measured with each experiment to control for day-to-day variation in camera sensitivity. The axial resolution (full width at half maximum) was 12.2 mm, measured with a ^{123}I line source in water in a cylindric phantom. ^{123}I-5-IA was synthesized as previously described (*31*) and administered through a venous catheter placed in the arm or hand using a bolus plus constant infusion with a ratio of 7.0 ± 0.02 h and a total injected dose (accounting for decay) of 361 ± 20 MBq. Another venous catheter was placed into the opposite arm or hand to collect blood for protein binding and metabolism. Previous data show that after 2 h of 5-IA infusion, venous and arterial samplings of the radiotracer are comparable (*32*). Therefore, we use venous sampling to obtain radiotracer protein binding and metabolism during the scanning period. Approximately 6 h after injection of ^{123}I-5-IA, a simultaneous transmission–emission scan and 3 equilibrium emission scans were obtained. Subjects were then removed from the camera, and a line was placed in the radial artery by an anesthesiologist after the Allen test was performed to assess collateral ulnar flow. An arterial catheter was used to collect blood for analysis of nicotine and its metabolite cotinine. The subjects were instructed to smoke up to 5 cigarettes of their preferred brand within 20 min, through a smoking topography device (Plowshare Technologies, Borgwaldt KC, Inc.) to control for any difference in puff volume. Because initial nicotine levels in arterial blood are higher than in venous samples (*33*), we collected arterial blood samples for the first 40 min of cigarette smoking, starting at the time of inhalation of the first cigarette, to determine nicotine and cotinine levels, after which venous samples were collected hourly until study completion. After the smoking challenge, one 30-min emission scan was acquired every hour for up to 6 h (all but 1 subject participated in all 6

TABLE 1. Demographic Variables and SPECT Scan Smoking Outcomes

Subject no.	Age (y)	Race	Sex	Cigarette		FTND	Days abstinent	Cigarettes smoked	T_{max} nicotine (min)	C_{max} nicotine (ng/mL)	Blood nicotine area under curve (60 min)
				Preferred brand)	Amount of nicotine						
1	22	Asian	Female	Parliament	0.7 mg	4.0	4.0	4.0	20.0	27.3	3,470.0
2	38	Caucasian	Male	Marlboro	1.0 mg	2.0	5.0	3.0	10.0	63.0	7,153.0
3	18	African American	Male	Newport	1.2 mg	8.0	6.0	2.0	5.0	45.0	7,840.0
4	50	Caucasian	Female	Rothmans	1.2 mg	2.0	4.0	2.5	2.0	112.0	27,700.0
5	54	Caucasian	Female	Virginia Slims	0.7 mg	8.0	6.0	2.5	10.0	45.4	4,488.0
6	54	Caucasian	Female	Marlboro	1.0 mg	10.0	5.0	1.5	5.0	54.2	9,767.0
7	20	Caucasian	Male	Marlboro	1.0 mg	7.0	4.0	2.0	2.0	65.0	4,864.0
8	48	Caucasian	Male	Newport	1.2 mg	6.0	6.0	2.0	5.0	38.0	3,764.0
9	39	Caucasian	Female	Parliament	0.7 mg	2.0	6.0	2.0	2.0	32.4	8,273.0
10	20	Hispanic	Male	Marlboro Smooth	1.0 mg	4.0	6.0	2.5	20.0	31.9	8,124.0
Mean ± SD	36.3 ± 15.0					5.3 ± 2.9	5.2 ± 0.9	2.4 ± 0.7	8.1 ± 6.9	51.4 ± 24.9	8,544.3 ± 7,068.8

FTND = Fagerstrom Test of Nicotine Dependence; T_{max} = time of maximum concentration of nicotine in blood; C_{max} = maximum concentration of nicotine in blood.

scans) to evaluate displacement of ^{123}I-5-IA from β_2*-nAChRs throughout the brain. Blood samples were collected at the midpoint of each postsmoking scan to quantify total parent and f_p, to correct for individual differences in metabolism and protein binding of ^{123}I-5-IA.

Image Analysis

SPECT emission images were analyzed as described previously (*21*). SPECT emissions were filtered using a 3-dimensional Butterworth filter (power factor, 10; cutoff, 0.24 cycle/pixel) and reconstructed using a filtered backprojection algorithm with a ramp filter on a 128 × 128 matrix to obtain 50 slices with a pixel size of 2.06 × 2.06 × 3.56 mm in the *x*-, *y*-, and *z*-axes. An attenuation map was reconstructed from the transmission and flood data, and nonuniform attenuation correction was performed (*34*). MR images were coregistered to each SPECT image to provide an anatomic guide for placement of standardized 2-dimensional regions of interest using MEDx software (Medical Numerics, Inc.). A 3-dimensional volume of interest was generated for each region and transferred to the coregistered SPECT image to determine regional radioactivity concentrations. The chosen regions of interest were those known to contain β_2*-nAChRs: the frontal, parietal, anterior cingulate, temporal, and occipital cortices; thalamus; striatum (an average of caudate and putamen); and cerebellum. Regional ^{123}I-5-IA uptake was determined by V_T/f_p, where V_T is brain regional activity divided by metabolite-corrected plasma activity and f_p is plasma parent. This measure is highly reproducible (*21*) and was previously designated as V_T, but the nomenclature was changed on the basis of a study by Innis et al. (*24*). Interrater variability, which was less than 10% across all regions, was computed as percentage difference between 2 raters using the equation $([V_{T\ 1}/V_{T\ 2}] - 1) \times 100$.

Determination of Receptor Occupancy and V_{ND}/f_p

V_T/f_P data, computed directly from the tissue and plasma radioactivity measurements from the presmoking baseline and postsmoking scans, were analyzed using Lassen plots. These plots have been validated by a recent study (*35*), with the equation for the line (y = rx + b), where y = (V_T/f_p [baseline] − V_T/f_p [after nicotine]), x = V_T (baseline), and linear regression of the fit to different brain regions provides receptor occupancy (r) and V_{ND}/f_p,

FIGURE 1. β_2*-nAChR occupancy plot based on Lassen method for representative subject's scan. Receptor occupancy by nicotine is determined from slope of linear regression (r), 74.4% in this case. V_{ND}/f_p is calculated as *y*-intercept divided by slope. For this scan, V_{ND}/f_p = 16.5 mL·cm^{-3}.

the y-intercept divided by the slope of the linear fit (Fig. 1). This approach assumes uniform receptor occupancy and a uniform level of V_{ND}/f_P (defined by Innis et al. (*24*)) across brain regions. Receptor occupancy and V_{ND}/f_P were thus derived for each subject across all brain regions for each postsmoking scan (compared with the presmoking baseline), and the final result represents the average across scans for each subject. We also derived V_{ND}/f_p without correcting for f_P to examine the role f_P plays in the derivation of V_{ND}/f_p.

Statistical Analysis

All statistical analyses were performed using SPSS (version 15.0; SPSS Inc.). Nonparametric correlational analyses (Spearman ρ-correlation coefficient) were used to examine the relationship between receptor occupancy and V_{ND}/f_p variables and smoking status. Statistical significance was set at P less than or equal to 0.05.

RESULTS

Mean total scores ± SD for the Fagerstrom Test of Nicotine Dependence (5.3 ± 2.8), Beck Depression Inventory (1.7 ± 1.7), and Center for Epidemiological Studies Depression Scale (4.8 ± 4.3) indicated that subjects were moderately dependent on tobacco and had negligible symptoms of depression during the study. At the time of screening, subjects had exhaled carbon monoxide levels (18.6 ± 6.1 pulses per minute) and plasma cotinine levels (228.2 ± 155.1 ng/mL) consistent with tobacco dependence. On the SPECT scanning day, subjects had low exhaled carbon monoxide (3.3 ± 3.8 pulses per minute) and plasma cotinine (55.0 ± 41.7 ng/mL) levels consistent with abstinence, as required for participation. After the set of baseline equilibrium scans, subjects smoked to satiety (mean cigarettes smoked ± SD, 2.4 ± 0.7). One subject showed abnormal nicotine metabolism after the smoking challenge. The typical pattern for nicotine availability in blood is to peak at approximately 10–20 min after smoke inhalation and subsequently to decrease over the next 1–2 h, depending on the amount of smoke inhalation and individual metabolism. On the basis of typical nicotine kinetics, we expected nicotine plasma levels to drop below detection levels (4 ng/mL) within 2–3 h after the smoking challenge. However, the excluded subject's nicotine levels in blood continued to rise through study completion, up to 6 h after cigarette smoking. This subject was excluded from subsequent analyses. For the rest of the subjects (1–10), after the smoking challenge the peak in nicotine levels was reached at 8.1 ± 6.9 min (Table 1) and maximum nicotine levels were 51.4 ± 24.9 ng/mL (Fig. 2B, representative subject).

f_p

The group mean and SD for f_p was 0.10 ± 0.04 (range, 0.6–1.6). Individual f_p values were used in subsequent calculations unless otherwise noted.

Receptor Occupancy

Equilibrium, operationally defined as less than a 5% change in receptor availability per hour ($mL \cdot cm^{-3} \cdot h^{-1}$), was reached between 6 and 8 h after injection (Fig. 2; representative subject, average change was 3.1%/h in the thalamus, 3.9%/h in the striatum, 0.1%/h in the mean cortex, and 2.7%/h in the cerebellum). After the smoking challenge (i.e., 2–5 h after smoking), there was minimal change in radiotracer binding (Table 2; Fig. 3), suggesting a pseudoequilibrium was reached, similar to a minimal change in binding a reported previously (3.1 h after smoking challenge) (*25*).

Peak occupancy of 69.1% ± 9.1% was reached at 3 h after the challenge. At 1 h after the challenge (i.e., 1 h from the start of smoking), maximum occupancy had not been reached, and at 6 h after the challenge, the receptor occupancy by nicotine started to decline (Table 2). Therefore, the data from scans 1 and 6 are not used in the derivation of final occupancy parameters. The decrease in β_2*-nAChR availability (or receptor occupancy by nicotine) after nicotine challenge was dramatic (Fig. 4; representative subject illustrated), with a maximal occupancy of 69.1% at 3 h after the smoking challenge and a range in receptor occupancy of 57.6%−69.1% over the 5-h scanning period for this subject. In the overall sample, the displacement of radiotracer by nicotine was 55%−80% across subjects and scans, with an average occupancy

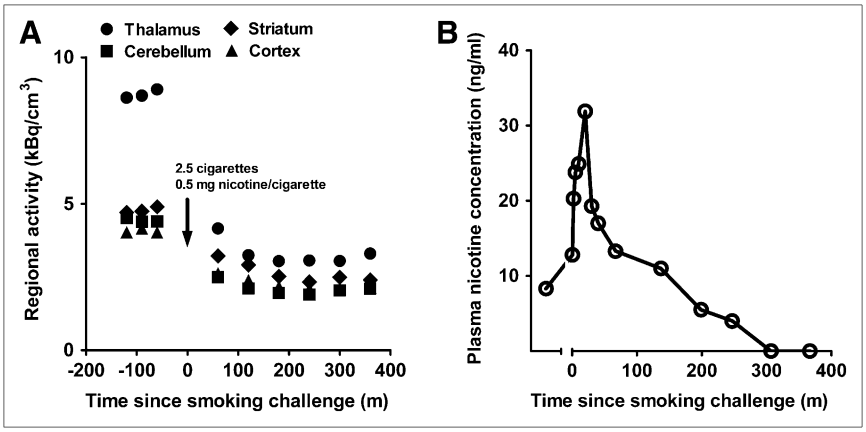

FIGURE 2. Time–activity curve (A) and associated blood plasma nicotine concentration (B) from representative subject. (A) Equilibrium was reached before subject had smoked to satiety: for this subject, average percentage change was 3.1%/h in thalamus, 3.9%/h in striatum, 0.1%/h in mean cortex, and 2.7%/h in cerebellum. Two to 5 h after smoker had smoked to satiety, there appeared to be little change in kBq/cm^3, suggesting that pseudoequilibrium state was achieved. (B) Highest nicotine concentration was observed at 20 min after initiation of tobacco smoking.

TABLE 2. Percentage Occupancy for Each Subject at 1–6 Hours After Smoking

	Time since smoking challenge							
Subject no.	1	2	3	4	5	6	Mean	SD
1	50.6	*62.6*	*63.7*	*64.6*	*N/A*	N/A	60.4	6.6
2	61.8	*70.4*	*80.6*	*80.7*	*72.7*	69.9	72.7	7.2
3	52.9	*56.3*	*59.0*	*60.8*	*56.0*	59.5	57.4	2.9
4	69.2	*79.5*	*82.9*	*79.9*	*79.1*	77.8	78.1	4.7
5	57.3	*65.7*	*71.7*	*66.5*	*60.9*	57.7	63.3	5.7
6	48.4	*54.2*	*63.9*	*57.1*	*54.1*	51.9	54.9	5.3
7	62.3	*71.4*	*69.8*	*64.1*	*62.1*	58.9	64.8	4.9
8	55.9	*59.0*	*59.7*	*66.2*	*72.0*	53.6	61.1	6.8
9	53.4	*56.8*	*61.1*	*62.0*	*59.6*	50.3	57.2	4.6
10	64.6	*80.4*	*78.9*	*76.3*	*78.4*	74.4	75.5	5.7
Mean	57.62	65.64	69.13	67.81	66.08	61.55	64.6	4.3
SD	6.67	9.51	9.05	8.25	9.57	10.05		

N/A = not applicable.

Italicized numbers are used to calculate final average receptor occupancy. Mean of receptor occupancy for scans between hours 2 and 5 after smoking challenge was used.

across scans 2–5 (2–5 h after the challenge) of 67.2% ± 9.1%.

V_{ND}/f_p

The estimates of V_{ND}/f_p remained stable over the course of the postsmoking challenge (Fig. 5), ranging from 15% to 28% across subjects, with an average of 19.4 ± 5.8 mL·cm^{-3} (SD of 27.6%) for V_{ND}/f_p. Thus, because baseline V_T/f_P in the thalamus was 93.5 mL·cm^{-3}, V_{ND}/f_p represents 20.7% of the activity in this region.

We also estimated nondisplaceable binding without correcting for f_p. Average V_{ND} was 7.03 ± 1.92 kBq/cm^3, and SD was 26.3%. Therefore, it does not appear that correction for plasma free fraction reduced the variability of nondisplaceable binding in this sample.

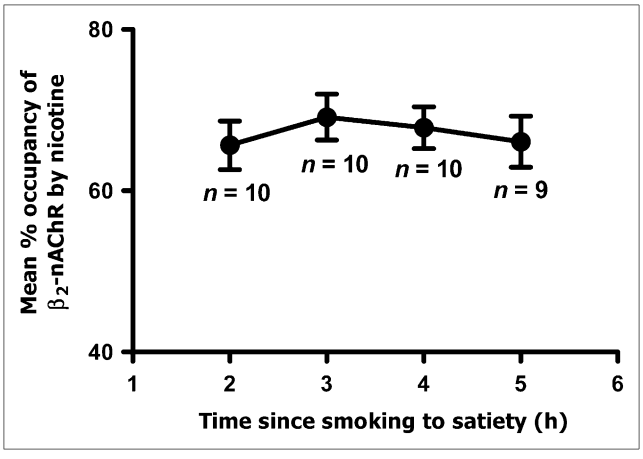

FIGURE 3. Percentage occupancy of β_2*-nAChRs by ^{123}I-5-IA (average and SEM) across all subjects after smokers had smoked to satiety. Receptor occupancy by nicotine remained relatively stable 2–5 h after smoking challenge.

Data Correlations

We examined if smoking variables play a role in receptor occupancy by nicotine or V_{ND}/f_p by conducting a nonparametric correlation analysis (Spearman ρ). We observed a positive correlation between number of cigarettes smoked on the scanning day (cigarette challenge to satiety) and receptor occupancy at hours 5 ($\rho = 0.67$, $P = 0.05$) and 6 ($\rho = 0.73$, $P = 0.03$) after challenge only (Fig. 6). There was no significant correlation between the number of cigarettes smoked on the scanning day and the average occupancy for hours 1–6 of scanning.

DISCUSSION

In the current study, we calculated β_2*-nAChR occupancy by nicotine by having human tobacco smokers smoke to satiety. Instead of saturating receptors with nicotine through alternate methods such as intravenous nicotine, having subjects smoke to satiation provides a more accurate quantification of receptor occupancy at the times that individuals are satisfied with their use of tobacco smoke. Consistent with a previous study (*25*), we demonstrated that in a typical tobacco smoker, most of the receptors remain occupied for a prolonged period. Specifically, in the current study, smoking an average of 2.4 cigarettes occupied up to 80% of receptors for up to 5 h; these results are comparable but somewhat lower than the previous report by Brody et al. (*1*), in which the receptor occupancy was 95% after subjects had smoked to satiety (2.8 cigarettes). One potential reason for this difference may be the method by which receptor occupancy was calculated. In the study by Brody et al., percentage occupancy was calculated as a ratio of receptors occupied after the challenge to receptors occupied before the challenge in each brain region and corrected for the amount of nicotine present in the subject's blood at the time of greatest occupancy (3.1 h)—typically less than 4 ng/mL. However, because there is no physiologic reason to assume differences in receptor occupancy across regions, we used the well-known Lassen method (*35*), previously used to calculate receptor occupancy. Further, because the lower limit of detection of nicotine in blood in our laboratory is 4 ng/mL and the half-life of nicotine is about 2.5 h, we were not able to correct for the amount of nicotine present in blood at the time of maximal occupancy.

As expected and consistent with a previous study (*25*), β_2*-nAChR occupancy was related to the number of cigarettes smoked on the scanning day (smoking-to-satiety challenge). We detected a significant positive correlation between receptor occupancy and the number of cigarettes smoked at challenge hours 5 and 6 of scanning only, suggesting that greater receptor occupancy was achieved by smoking a greater number of cigarettes.

We also determined the magnitude of V_{ND}/f_p (sum of nonspecific and free) for ^{123}I-5-IA for the first time, to our knowledge, in human subjects. This determination was

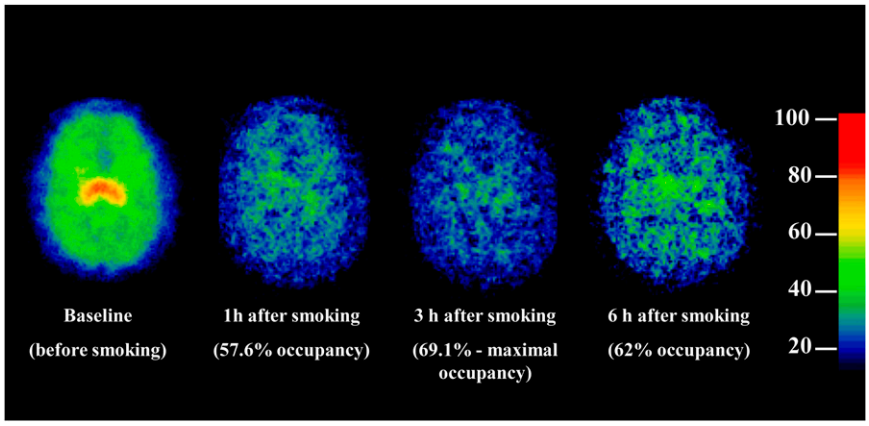

FIGURE 4. Parametric image of β_2-nAChR availability in representative subject before and after smokers had smoked to satiety (20-y-old man; 2.4 cigarettes). Maximal occupancy was not reached until approximately 3 h after smoking. By 6 h after smoking, the receptor occupancy by nicotine was reduced. Color scale is shown with red, yellow, green, and blue corresponding to values of regional activity divided by free plasma parent (V_T/f_p).

made by having tobacco smokers smoke to satiety (*36*). In addition, the current study was conducted exclusively in subjects who were habitual smokers because administration of saturating doses of nicotine to nicotine-naïve subjects can have serious side effects and also raises the ethical issue of giving drugs to drug-naïve individuals (*37*). We determined that, at baseline, V_{ND}/f_p represents about 20% of total ^{123}I-5-IA binding in the thalamus, the mostly densely populated β_2*-nAChR region. We observed between-subject variability in V_{ND}/f_p, which is likely due to individual differences in nonspecific binding and free radiotracer concentration in the brain as measured with ^{123}I-5-IA SPECT. We did not observe significant variability in V_{ND}/f_p across the 6-h scanning period, suggesting that the full 6-h block is not necessary to measure V_{ND}/f_p. However, here we used the average across all 6 scans to report mean group V_{ND}/f_p that may be used to obtain a more precise measure of receptor availability in future studies. Further, although determining the magnitude of nondisplaceable binding for ^{123}I-5-IA correction for f_p may not be necessary, because of population differences in f_p, this correction is important. Previous reports in nonhuman primates estimated specific binding to be at about 70% in the thalamus; thus, nondisplaceable binding (specific and free) would be about 30%, which is slightly higher than the percentage in the current sample (*19*). The current results will allow future studies to determine β_2*-nAChR availability more accurately.

There are several limitations to the current study. First, the finite dissociation and brain clearance of ^{123}I-5-IA from the receptor–ligand complex limits the use of ^{123}I-5-IA, or any radioligand, and neuroreceptor imaging techniques (*8,11,38*). Finite dissociation and brain clearance mean that the radioligand binding to the receptor does not instantaneously match the available receptor. Further, even if the ligand dissociates from the receptor because of competition (e.g., from drug), this tracer must leave the brain to detect a change in the imaging signal. In the case of nicotine, tobacco smoke enters the body through the mouth, is inhaled into the lungs, and is then absorbed into the circulatory system that delivers it to the brain. When delivered this way to dependent smokers, nicotine from tobacco smoke reaches the brain within approximately 30 s of inhalation (*39*). A typical tobacco smoker requires approximately 5 min to smoke a cigarette. With nicotine's half-life of approximately 90 s in the lungs, and with the brain uptake being highly correlated with rate of washout from the lung (*39*), it is probable that the maximal brain concentration and receptor occupancy are reached much earlier than measured by ^{123}I-5-IA, because it takes ^{123}I-5-IA quite some time to dissociate from the receptor and exit the brain. In fact, by 3 h after smoking, the occupancy by nicotine may have dropped enough so that ^{123}I-5-IA uptake levels begin to rebound.

A second potential limitation to studying the nAChRs using A-85380 is that endogenous acetylcholine competes

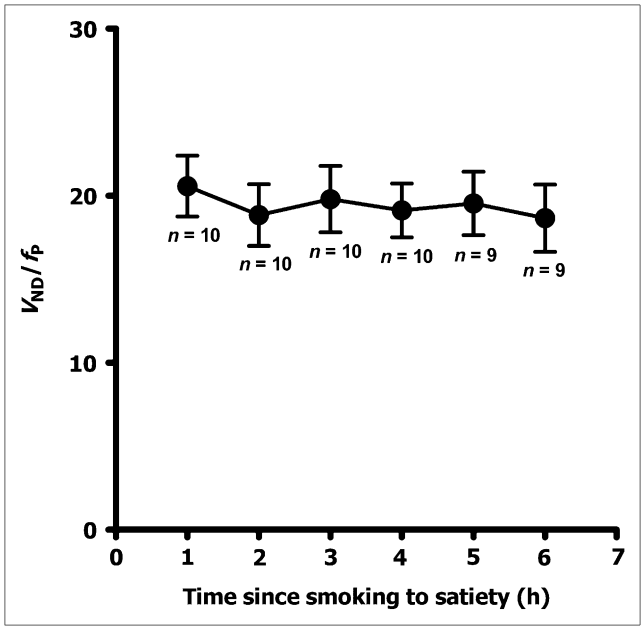

FIGURE 5. Illustration of nondisplaceable uptake after smoking to satiety across all subjects for each scanning time. Nondisplaceable uptake remained relatively stable over 6-h scanning period, suggesting it was stable when receptors were saturated. Error bars represent SEM.

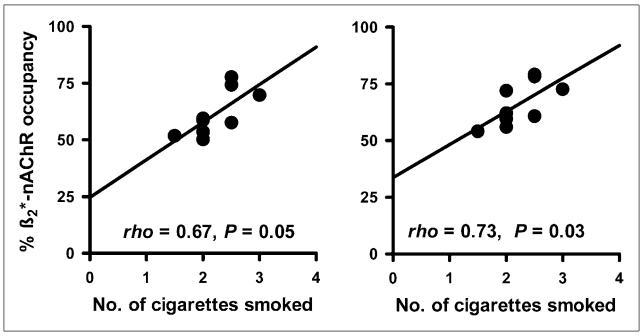

FIGURE 6. Percentage occupancy of β_2*-nAChRs at hours 5 and 6 after smokers had smoked to satiety significantly correlated with number of cigarettes smoked at challenge (hour 5: $\rho = 0.67$, $P = 0.05$, and hour 6: $\rho = 0.73$, $P = 0.03$).

with ^{123}I-5-IA for binding to nAChRs (*39*). Fujita et al. (*40*) showed that ^{123}I-5-IA was displaced by increased levels of acetylcholine, and the change in 5-IA levels was caused by a change in specific, not nonspecific, binding. This means that an increase in baseline levels of acetylcholine occupancy will decrease the binding of ^{123}I-5-IA, a potentially relevant finding in the current study because some of the receptors may be occupied by acetylcholine and not available for nicotine or the radioligand. In this case, the baseline V_T/f_P values, and the magnitude of occupancy by nicotine, will be underestimated. The low variance between occupancy measures across subjects suggests that despite different numbers of cigarettes smoked, β_2*-nAChR occupancy is a reasonably good imaging biomarker, relevant to behavioral states in the subject.

Third, these findings may not generalize to psychiatric populations. Though it is likely that there are no significant differences in V_{ND}/f_p between populations, we cannot state with confidence that the V_{ND}/f_p as reported here is appropriate to use in psychiatric populations without further study. We are currently evaluating β_2*-nAChR availability in psychiatric populations, including smokers with schizophrenia and alcohol-use disorders. Future work will need to examine whether V_{ND}/f_P is uniform among psychiatric populations, as compared with healthy controls, to ensure that the differences in receptor binding are not due to differences in V_{ND}/f_p. Presently, the V_{ND}/f_p value as calculated here may be used with caution when reporting V_S/f_p in psychiatric populations. Because V_{ND}/f_p accounts for approximately 20% only of thalamic binding, a large between-group change in V_{ND}/f_p would be needed to affect the interpretation of between-group differences in V_T/f_p.

CONCLUSION

To date, no neuroimaging studies using ^{123}I-5-IA report calculations of V_{ND}/f_p. Presently, we demonstrate that receptor occupancy by nicotine from satiating tobacco smoke levels reaches a maximum at 2–5 h after nicotine challenge, which is somewhat contradictory to smokers' self-report of craving tobacco smoke every 1–2 h. We propose that one of the reasons for this discrepancy is the slow kinetics of ^{123}I-5-IA and that the maximal receptor occupancy by nicotine after use of a cigarette might be reached more quickly. In future studies, we plan to examine the relationship between nicotine occupancy of β_2*-nAChR and tobacco smoke craving, urges, and withdrawal to better understand other aspects of cigarette smoking that may contribute to frequent daily use of cigarettes.

Further, we calculated nondisplaceable uptake of ^{123}I-5-IA (V_{ND}/f_p) and demonstrated that it was approximately 20% of total binding for this radiotracer in the thalamus of healthy human smokers. This finding suggests that ^{123}I-5-IA is an excellent tracer to continue the investigation of β_2*-nAChR in vivo. Further, this study provides a more precise measurement of β_2*-nAChR availability in vivo, and β_2*-nAChR should be considered in future studies using ^{123}I-5-IA for a more accurate measure of V_T/f_p.

ACKNOWLEDGMENTS

We thank Louis Amici for radiochemistry and Marina Picciotto for her intellectual contribution. We also thank Gina Nicoletti, Andrea Perez, and Jane Bartosik for technical support. This research was supported in part by National Institute of Health grants KO2 DA21863, P50 AA15632, KO1 DA20651, T32 DA07238-16, and VA CDA-1. The content is solely the responsibility of the authors and does not necessarily represent the official views of the National Institute on Alcohol Abuse and Alcoholism, the National Institute on Drug Abuse, or the National Institutes of Health. This article was written in memory of Julie K. Staley, Ph.D.

REFERENCES

1. Brody A, Mandelkern M, Costello M, et al. Brain nicotinic acetylcholine receptor occupancy: effect of smoking a denicotinized cigarette. *Int J Neuropsychopharmacol.* 2009;12:305–316.
2. Cosgrove K, Batis J, Bois F, et al. β2-Nicotinic acetylcholine receptor availability during acute and prolonged abstinence from tobacco smoking. *Arch Gen Psychiatry.* 2009;66:666–676.
3. Griffith J, O'Neill J, Petty F, Garver D, Young D, Freedman R. Nicotinic receptor desensitization and sensory gating deficits in schizophrenia. *Biol Psychiatry.* 1998;44:98–106.
4. Breese C, Lee M, Adams C, et al. Abnormal regulation of high affinity nicotinic receptors in subjects with schizophrenia. *Neuropsychopharmacology.* 2000;23:351–364.
5. Court J, Martin-Ruiz C, Piggott M, Spurden D, Griffiths M, Perry E. Nicotinic receptor abnormalities in Alzheimer's disease. *Biol Psychiatry.* 2001;49:175–184.
6. Ellis J, Villemagne V, Nathan P, et al. Relationship between nicotinic receptors and cognitive function in early Alzheimer's disease: a 2-[^{18}F]fluoro-A-85380 PET study. *Neurobiol Learn Mem.* 2008;90:404–412.
7. Abreo M, Lin N-H, Garvey D, et al. Novel 3-pyridyl ethers with subnanomolar affinity for central neuronal nicotinic acetylcholine receptors. *J Med Chem.* 1996;39:817–825.
8. Vaupel D, Mukhin A, Kimes A, Horti A, Koren A, London E. *In vivo* studies with [^{125}I]5-IA 85380, a nicotinic acetylcholine receptor radioligand. *Neuroreport.* 1998;9:2311–2317.

9. Horti A, Chefer S, Mukhin A, et al. 6-[^{18}F]fluoro-A-85380, a novel radioligand for in vivo imaging of central nicotinic acetylcholine receptors. *Life Sci.* 2000; 67:463–469.
10. Chefer S, Horti A, Koren A, et al. 2-[^{18}F]F-A-85380: a PET radioligand for $\alpha_4\beta_2$ nicotinic acetylcholine receptors. *Neuroreport.* 1999;10:2715–2721.
11. Mukhin A, Gundisch D, Horti A, et al. 5-Iodo-A-85830, an a4b2 subtype-selective ligand for nicotinic acetylcholine receptors. *Mol Pharmacol.* 2000;57: 642–649.
12. Villemagne V, Horti A, Scheffel U, et al. Imaging nicotinic acetylcholine receptors with fluorine-18-FPH, an epibatidine analog. *J Nucl Med.* 1997;38: 1737–1741.
13. Musachio J, Villemagne V, Scheffel U, et al. [125/^{123}I]IPH: a radioiodinated analog of epibatidine for in vivo studies of nicotinic acetylcholine receptors. *Synapse.* 1997;26:392–399.
14. Nordberg A, Alafuzoff I, Winblad B. Nicotinic and muscarinic subtypes in the human brain: changes with aging and dementia. *J Neurosci Res.* 1992;31:103–111.
15. Swanson L, Simmons D, Whiting P, Lindstrom J. Immunohistochemical localization of neuronal nicotinic receptors in the rodent central nervous system. *J Neurosci.* 1987;7:3334–3342.
16. Koren A, Horti A, Mukhin A, et al. 2-, 5-, and 6-Halo-3-(2(*S*)-azetidinylmethoxy)pyridines: synthesis, affinity for nicotinic acetylcholine receptors, and molecular modeling. *J Med Chem.* 1998;41:3690–3698.
17. Fujita M, Seibyl J, Vaupel D, et al. Whole body biodistribution, radiation-absorbed dose and brain SPET imaging with [^{123}I]5-I-A-85830 in healthy human subjects. *Eur J Nucl Med.* 2002;29:183–190.
18. Vaupel DB, Tella SR, Huso DL, et al. Pharmacological and toxicological evaluation of 2-fluoro-3-(2(S)-azetidinylmethoxy)pyridine (2-F-A-85380), a ligand for imaging cerebral nicotinic acetylcholine receptors with positron emission tomography. *J Pharmacol Exp Ther.* 2005;312:355–365.
19. Fujita M, Tamagnan G, Zoghbi S, et al. Measurement of a_4b_2 nicotinic acetylcholine receptors with [^{123}I]5-I-A85830 SPECT. *J Nucl Med.* 2000;41: 1552–1560.
20. Chefer S, Horti A, Lee K, et al. In vivo imaging of brain nicotinic acetylcholine receptors with 5-[^{123}I]iodo-A-85830 using single photon emission computed tomography. *Life Sci.* 1998;63:PL355–PL360.
21. Staley JL, van Dyck C, Weinzimmer D, et al. Iodine-123-5-IA-85380 SPECT measurement of nicotinic acetylcholine receptors in human brain by the constant infusion paradigm: feasibility and reproducibility. *J Nucl Med.* 2005;46:1466–1472.
22. Ding Y, Fowler J, Logan J, et al. 6-[^{18}F]Fluoro-A-85380, a new PET tracer for the nicotinic acetylcholine receptor: studies in the human brain and in vivo demonstration of specific binding in white matter. *Synapse.* 2004;53:184–189.
23. Cosgrove K, Mitsis E, Bois F, et al. ^{123}I-5-IA-85380 SPECT imaging of nicotinic acetylcholine receptor availability in nonsmokers: effects of sex and menstrual phase. *J Nucl Med.* 2007;48:1633–1640.
24. Innis R, Cunningham V, Delforge J, et al. Consensus nomenclature for in vivo imaging of reversibly binding radioligands. *J Cereb Blood Flow Metab.* 2007;27: 1533–1539.
25. Brody A, Mandelkern M, London E, et al. Cigarette smoking saturates brain $\alpha_4\beta_2$ nicotinic acetylcholine receptors. *Arch Gen Psychiatry.* 2006;63:907–915.
26. Soria R, Stapleton J, Gilson S, Sampson-Cone A, Henningfield J, London E. Subjective and cardiovascular effects of intravenous nicotine in smokers and non-smokers. *Psychopharmacology (Berl).* 1996;128:221–226.
27. Perkins KA, Grobe J, Epstein L, Caggiula A, Stiller R, Jacob R. Chronic and acute tolerance to subjective effects of nicotine. *Pharmacol Biochem Behav.* 1993;45:375–381.
28. Newhouse PA, Sunderland T, Narang P, et al. Neuroendocrine, physiologic, and behavioral responses following intravenous nicotine in nonsmoking healthy volunteers and in patients with Alzheimer's disease. *Psychoneuroendocrinology.* 1990;15:471–484.
29. American Psychiatric Association. *Diagnostic and Statistical Manual of Mental Disorders: DSM-IV.* 4th ed. Washington, DC: American Psychiatric Association; 1994.
30. Staley JK, Krishnan-Sarin S, Cosgrove K, et al. Human tobacco smokers in early abstinence have higher levels of β_2* nicotinic acetylcholine receptors than nonsmokers. *J Neurosci.* 2006;26:8707–8714.
31. Zoghbi S, Tamagnan G, Fujita M, et al. Measurement of plasma metabolites of (*S*)-5-[^{123}I]iodo-3-(2-azetidinylmethoxy)pyridine (5-IA-85380), a nicotinic acetylcholine receptor imaging agent, in non-human primates. *Nucl Med Biol.* 2001; 28:91–96.
32. Mamede M, Ishizu K, Udea M, et al. Quantification of human nicotinic acetylcholine receptors with ^{123}I-5IA SPECT. *J Nucl Med.* 2004;45:1458–1470.
33. Henningfield JE, Stapletom J, Benowitz N, Grayson R, London E. Higher levels of nicotine in arterial than in venous blood after cigarette smoking. *Drug Alcohol Depend.* 1993;33:23–29.
34. Rajeevan N, Zubal I, Rambsy S, Zoghbi S, Seibyl J, Innis R. Significance of nonuniform attenuation correction in quantitative brain SPECT imaging. *J Nucl Med.* 1998;39:1719–1726.
35. Cunningham V, Rabiner E, Slifstein M, Laruelle M, Gunn R. Measuring drug occupancy in the absence of a reference region: the Lassen plot re-visited. *J Cereb Blood Flow Metab.* 2010:30:46–50.
36. Drugs.com. Nicotine Side Effects. Available at: http://www.drugs.com/sfx/nicotine-side-effects.html. Accessed April 27, 2010.
37. Perkins KA, Coddington S, Karelitz J, et al. Variability in initial nicotine sensitivity due to sex, history of other drug use, and parental smoking. *Drug Alcohol Depend.* 2009;99:47–57.
38. Endres CJ, Carson R. Assessment of dynamic neurotransmitter changes with bolus or infusion delivery of neuroreceptor ligands. *J Cereb Blood Flow Metab.* 1998;18:1196–1210.
39. Muhkin A, Garg P, Lokitz S, et al. Comparison of brain nicotine accumulation after cigarette smoking in dependent and non-dependent smokers [abstract]. *J Nucl Med.* 2008;49(suppl 1):234P.
40. Fujita M, Al-Tikriti M, Tamagnan G, et al. Influence of acetylcholine levels on the binding of a SPECT nicotinic acetylcholine receptor ligand [^{123}I]5-I-A-85380. *Synapse.* 2003;48:116–122.